

NOTATION

T_1 , C_1 , a_1 , λ_1 , γ_1 , solid-phase temperature, specific heat, thermal diffusivity, thermal conductivity, and density; T_2 , λ_2 , γ_2 , liquid temperature, thermal conductivity, and density; r_0 , siphon outside radius; D_0 , siphon outside diameter; r_f , radius of phase transition front; D_{ic} , ice column diameter; k , effective siphon heat-transfer coefficient; T_a , T_{wa} , T_w , air temperature, water temperature around evaporative part, and temperature at outer surface of siphon correspondingly; T_f , phase-transition temperature; α_f , heat-transfer coefficient from water to phase-transition surface; L , latent heat of fusion; t_f , time required to produce ice of a given thickness on a siphon.

LITERATURE CITED

1. P. A. Vislobitskii, A. P. Klimenko, A. I. Titarenko, and Yu. N. Shirikhin, *Stroit. Trubopr.*, No. 2, 29-30 (1982).
2. E. S. Kurylev, V. V. Onosovskii, and V. S. Sokolov, *Kholodil'naya Tekh.*, No. 6, 37-41 (1974).
3. N. A. Buchko, I. K. Lebedkina, et al., *Kholod. Tekh.*, No. 3, 25-27 (1976).
4. Hidetoshi Aoki et al., *Ref. Zh. Mekh.*, No. 6, Ref. 7B 580 (1980).
5. J. M. Dumore et al., *Nature*, 172, No. 4375, 460-461 (1953).
6. V. M. Gorislavets and L. P. Semenov, *Inzh.-Fiz. Zh.*, 48, No. 4, 610-617 (1985).
7. A. A. Samarskii, *Introduction to Difference-Scheme Theory* [in Russian], Moscow (1977).
8. P. F. Fil'chakov, *Numerical and Graphical Methods in Applied Mathematics* [in Russian], Kiev (1970).
9. A. V. Lykov, *Thermal Conductivity Theory* [in Russian], Moscow (1951).
10. E. M. Sparrow et al., *Teploperedacha*, No. 4, 1-9 (1979).
11. *Instructions on Building Technology for Ice Crossings Frozen by Means of Two-Phase Thermal Siphons in the Construction of Major Pipelines* [in Russian], VSN 175-84, Minneftegazstroj, Moscow (1985).

PROPERTIES OF NONSTEADY-STATE HEAT TRANSFER TO SUPERFLUID HELIUM

V. M. Miklyaev, I. A. Sergeev,
and Yu. P. Filippov

UDC 536.48

Results are presented from an experimental study of heat transfer from a cylindrical specimen to a volume of superfluid helium with thermal loading in the form of an impulsive step. Unique features of He II as a cooling agent as compared to He I are noted and discussed.

In recent years the number of studies dedicated to heat transport and hydrodynamics of superfluid helium has increased significantly. This is due, first, to the need to construct an adequate heat transport theory [1], and second, to the possibility of practical use of He II as a cooling agent in cryogenic systems [2, 3]. In particular, the literature offers experimental data concerning the physics of the superfluid liquid (its hydrodynamics, acoustics, phase transitions) [4, 5] and processes occurring on a solid body-He II boundary (Kapitsa resistance, critical thermal flux, heat transport in various regimes) [6, 7]. However, as was noted in the review [1], questions of nonsteady state heat transfer to He II, the development of thermal perturbations with a turbulent front, and the dynamics of He II \rightarrow He vapor and He II \rightarrow He I phase transitions require additional study.

The goal of the present study is to investigate the processes of nonsteady-state heat transfer from the surface of a solid body of cylindrical form immersed in superfluid helium.

The experiments were performed in He II upon the free surface of which a pressure $P_s = 1780$ Pa was maintained (equilibrium temperature $T_s = 1.82$ K). The helium II volume $\approx 3.0 \cdot 10^{-3}$ m³, the free liquid surface area $\approx 1.54 \cdot 10^{-2}$ m², specimen immersion depth 0.05-0.15 m.

Joint Institute for Nuclear Research, Dubna. Translated from *Inzhenerno-Fizicheskiy Zhurnal*, Vol. 54, No. 6, pp. 950-956, June, 1988. Original article submitted February 6, 1987.

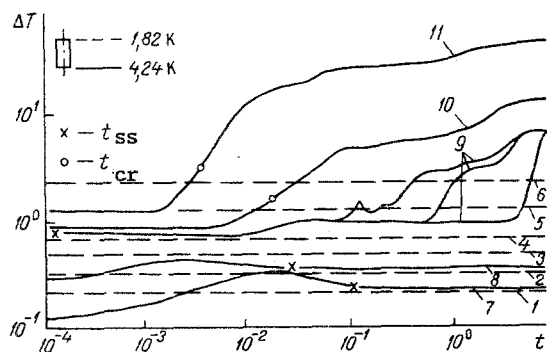


Fig. 1

Fig. 1. Surface temperature rise ΔT , K, vs time t , sec, after application of power pulse W , $W - \Delta T(t)_W$ - for vertical specimen orientation in free flow conditions in He II and He I [8]: 1) $W = 0.08$ W; 2) 0.15; 3) 0.31; 4) 0.61; 5) 2.4; 6) 9.8; 7) 0.34; 8) 1.4; 9) 7.7; 10) 9.7 W; 11) 19.7 W. (Results obtained in He II with horizontal orientation were practically identical.)

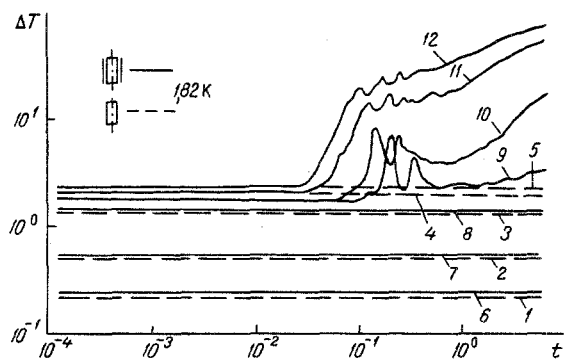


Fig. 2

Fig. 2. Functions $\Delta T(t)_W$ for vertical specimen orientation under free and restricted flow conditions in helium II: 1) $W = 0.08$ W; 2) 0.3; 3) 2.4; 4) 7.6; 5) 9.8; 6) 0.08; 7) 0.32; 8) 2.4; 9) 4.5; 10) 5.3; 11) 7.8; 12) 10 W.

The specimen was a polished ceramic tube $\emptyset 11.5 \times 1.75$ mm, on the outer surface of which a carbon film 54 mm long was deposited [8]. The ceramic tube was evacuated and its ends sealed with glued cover end caps. The carbon film served simultaneously as a heater and a low inertia high sensitivity thermoconverter. The thickness of this heater-thermometer was less than $1 \mu\text{m}$, with thermal reaction time less than 100 nsec, and sensitivity $\left| \frac{1}{R} \frac{dR}{dT} \right|$ of about 0.65 K^{-1} at a temperature of 1.8 K and about 0.20 K^{-1} at 4.0 K.

Studies were performed with both horizontal and vertical orientation under both free and restricted flow conditions. The latter was modelled by placing the specimen coaxially within a steel tube $\emptyset 16 \times 1.0$ mm, 80 mm long, such that an annular gap 1.25 mm wide was formed between the heater-thermometer surface and the inner surface of the tube.

Thermal loading was applied to the heater-thermometer in the form of a step pulse, with risetime of not more than 10 μsec , while the equipment insured time stability of the heat power liberated in the heater-thermometer. The drift in heat liberation did not exceed 2% of the mean power level W . A block diagram and description of the electronic equipment used, which operated in conjunction with a MERA-60 computer, were presented in [8].

The experimental results were processed in the form of dependences of the integral heating of the heater-thermometer $\Delta T = T - T_s$ on time t after application of the power pulse $\Delta T(t)_W$. Each $\Delta T(t)_W$ curve consisted of 4736 points, of which 4096 were obtained with a time resolution of 50 μsec while the remainder were obtained at 10 msec intervals with a repeated pulse of the same power level. The first measurement was performed 10 μsec after application of the pulse to the heater. The intervals between measurements were controlled to an accuracy of not less than 1 μsec . The uncertainty in determining the temperature rise did not exceed 10 mK for $\Delta T < 3.5$ K, and was not more than 0.5% in the remaining range. The uncertainty in measurement of liberated heat power comprised 1-4%, with the higher value occurring at lower W levels.

All the data and computation expressions available in the literature on the characteristics of nonsteady state processes in He II were obtained for one-dimensional geometry (long narrow channels [3, 5]). In the present study the experimental geometry was either two-dimensional (vertical orientation) or three-dimensional (horizontal). As for steady state regimes, practically all data has been obtained for either plates or thin filaments. The parameters of the present specimen - outer diameter, area of the heat liberating surface - exceed the corresponding parameters of the specimens of a majority of other authors by one to two orders of magnitude. In view of this it is difficult to use quantitative information from the literature as a departure point for the study. Therefore, the experiments were

TABLE 1. Characteristics of Temperature Rise Peaks for Various Orientations and Thermal Loads

Orientation	W, W	Peak 1			Peak 2			Peak 3		
		τ , msec	A, K	G, msec	τ , msec	A, K	G, msec	τ , msec	A, K	G, msec
Vertical	3,9	260	4,00	40	370	1,50	45	—	—	—
	4,5	195	5,20	30	330	1,90	60	—	—	—
	5,3	145	4,60	40	235	3,10	55	—	—	—
Horizontal	3,9	265	4,35	35	415	4,00	45	555	3,10	45
	4,2	230	4,40	40	380	6,10	30	530	4,00	40
	4,3	240	3,90	50	420	4,00	65	545	4,15	75

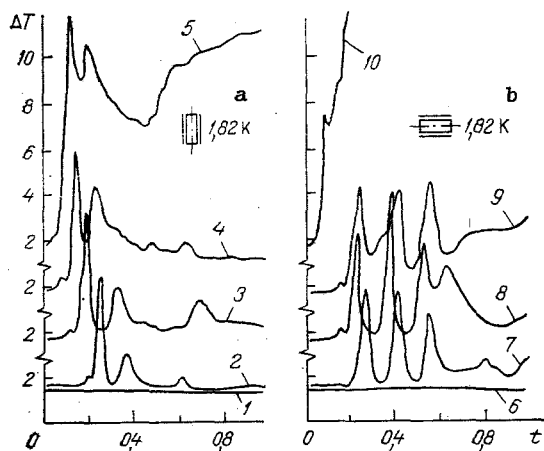


Fig. 3. Functions $\Delta T(t)_W$ in transition region for vertical (a) and horizontal (b) specimen orientations under restricted flow conditions: 1) $W = 3.1$ W; 2) 3.9; 3) 4.5; 4) 5.3; 5) 6.8; 6) 3.1; 7) 3.9; 8) 4.2; 9) 4.3; 10) 6.6 W. (For better distinction between the curves the ordinate axis is interrupted at the 2.0 mark.)

performed for the same time and thermal load G , ranges as were used in previous studies in an He I volume with the same specimen [8].

Data were obtained for temperature increases of 0.1-100 K with times of 10 μ sec-6.4 sec, pulse powers of 0.08-10 W (which corresponds to thermal flux densities in the helium of $q \approx 40$ -5000 $W \cdot m^{-2}$).

The experimental results indicate some quite unique features of nonsteady state heat transport to He II, as compared to He I, as is shown in Fig. 1. To discuss these features, we must first consider a characteristic of nonsteady state heat transport, the time t_{SS} . The value of t_{SS} is determined by the time over which for thermal loads less than critical steady state heat removal regimes are established (curve 7 for $t > 100$ msec; curve 8 for $t > 20$ msec), or the time for establishment of metastable regimes for loads exceeding critical (curve 9 for 0.1 msec $< t < 6$ msec).* In normal helium the time t_{SS} is related to the moment when the thermal conductivity heat liberation regime in helium I is replaced by bubble (steady state or metastable) boiling. The value of t_{SS} is then strictly related to the thermal load and comprises ≈ 100 msec for $W = 0.34$ W (curve 7), ≈ 20 msec for 1.4 W (curve 8), and ≈ 0.1 msec for 7.7 W (curve 9). In contrast to this, in He II over the entire load interval studied t_{SS} was no greater than 0.1 msec. This fact may be related to the extremely rapid achievement of a value of the Kapitza conductivity h corresponding to the applied thermal load. According to the data of [9], values of h obtained by the steady state method and the second sound method coincide. The maximum frequency of the change in loading in [9] comprised 600 Hz, i.e., under the conditions of those experiments the Kapitza regime was established over a time of less than 1 msec. In the first approximation this agrees with the current results. Thus, the first unique feature of nonsteady state heat transport to He II is that the quantity t_{SS} is at least three orders of magnitude (judging from curves 3 and 7) lower than t_{SS} for helium I at the same thermal load.

The second feature is related to the very long time required for onset of the crisis,†

* In Fig. 1 the times of establishment of steady state and metastable regimes are denoted by the symbol x .

† In Fig. 1 the onset of the crisis is denoted by the symbol o . (The time of the crisis was identified by the generally used method - an excess in the temperature rise of 30% of the ΔT value in the metastable nucleation regime.)

t_{cr} , upon which a transition to film boiling occurs. For He I the value of t_{cr} comprises tens of msec for $W = 9.7$ (curve 10) and units of msec for 19.7 W (curve 11), while for helium II under free circulation conditions over the entire range of times and loads studied the crisis phenomenon was not observed, although a portion of the data (line 6) was obtained at specific pulse powers exceeding the steady-state critical value q_{cr} . As will be shown below, under confined conditions with such loads there is a transition to film boiling, but, as is well known [10], q_{cr} does not depend on the size of the channel in the He II. In all probability the absence of a crisis indicates that over the measurement period (6.4 sec) the temperature t_{cr} was not reached in the superfluid helium. This is supported by a calculation of t_{cr} using the relationship:

$$t_{cr} = B(T)q^{-4}, \quad (1)$$

where q is the thermal flux density, $B(T)$ is a constant depending on the helium temperature T_* ($B \approx 100 \text{ W}^4 \cdot \text{cm}^{-8} \cdot \text{sec}$). According to Eq. (1), which has been obtained both empirically [3] and theoretically [11], under the conditions of the present experiments t_{cr} is of the order of magnitude of tens of minutes at a load of 9.8 W, which does not contradict the results presented. Thus, the value of t_{cr} for helium II is at least three orders of magnitude larger (judging from curves 6 and 10) than t_{cr} for helium I at the same loads.

Moreover, the processes recorded in nonsteady state heat transport within the superfluid helium volume are not characterized by the instability region which is found under analogous conditions in normal helium [8]. The instability region is formed by $\Delta T(t)_W$ curves corresponding to pulse powers close to the steady state critical value, and is found in the temperature rise range of $\approx 1-10$ K with times of $\approx 0.1-10$ sec. The temperature rise and time ranges in which the instability region is found depend on orientation and experimental conditions [8]. In the instability region a number of nonlinear effects were observed [8], in particular, branching of the $\Delta T(t)_W$ curves (see, for example, curve 9). Since for He I the causes of formation of this region are closely related to the crisis phenomenon, it can be proposed that for He II a similar region does not manifest itself due to the insufficient duration of the measurement period (the time t_{cr} was not reached).

In the presence of an annular gap around the heater-thermometer the character of nonsteady state heat transport into superfluid helium partially retains the unique features noted above, but a number of qualitatively different processes are observed.

The results obtained in a helium II volume ($P_s = 1780$ Pa) for vertical orientation of the specimen under restricted flow conditions are represented by curves 6-12 of Fig. 2, where for comparison data for free flow conditions are also shown (lines 1-5). It is evident from the figure that at loads less than some critical value, there are only slight quantitative differences between the results for free and restricted conditions. However, for pulse powers exceeding this value there are qualitative differences, which are illustrated by curves 9-12, which form a specific region for temperature rises of $\approx 1.35-35$ K and times ≈ 500 msec-6.4 sec. Below we will call this region the "transition region." At first glance this transition region recalls the instability region found for He I; however, as will be shown below, the reason for development of this region and the character of the processes occurring therein are completely different. After these processes there may occur (if the value q_{cr} is exceeded) a transition to film boiling, as is indicated by the stable (for the course of ≈ 6 sec) growth in specimen surface temperature rise up to values of $\Delta T \approx 100$ K (curves 11 and 12).

Change in orientation of a specimen located under restricted conditions from vertical to horizontal, on the one hand, produces no principal changes in the overall pattern of nonsteady state heat transport in He II. Thus, for horizontal orientation, we also find a transition region and transitions to film boiling, with the pulse power value and time and load intervals in which the transitions are located coinciding with the corresponding quantities for vertical orientation. But on the other hand, the paths of the $\Delta T(t)_W$ curves show differences which are presented in Fig. 3.

It is evident from Fig. 3a that for vertical orientation in the transition region two temperature peaks can be identified. The characteristics of these peaks, the amplitude A , half-width G , and time of onset τ , change monotonically with increase in load. However, for horizontal orientation we see three peaks, with characteristics depending on load more weakly (Fig. 3b). The values of A , G , τ for various loads W are presented in Table 1. It should be noted that the reproducibility of these data in the transition region is practically complete.

The existence of transition regions and the characteristics of the processes occurring therein under restricted flow conditions can be explained in the following manner. The development of the first temperature peak is probably caused by turbulization of the superfluid component of the He II in the annular channel around the heater-thermometer surface. This is confirmed by the satisfactory agreement between the times at which the first peaks occur τ with the vortex formation times t_{vx} in He II, calculated with the expression [5]:

$$t_{vx} = C(T)q^{-\frac{3}{2}}, \quad (2)$$

where $C(T)$ is an empirical constant, which depends on the channel geometry and the helium temperature T and is of the order of magnitude of $0.1 \text{ W}^{3/2} \cdot \text{cm}^{-3} \cdot \text{sec}$. In this sense the threshold load $\approx 3.1 \text{ W}$ (lines 1 and 6) corresponds to steady critical vortex formation flux q_{vx} . We note that the value obtained for q_{vx} is approximately an order of magnitude higher than the value of $10\text{-}100 \text{ W} \cdot \text{m}^{-2}$ of the steady state critical vortex formation flux known for long narrow channels [1, 4].

Immediately thereafter the turbulized helium layer rapidly heats through, which can lead to a phase transition of metastable liquid helium II \rightarrow metastable liquid helium I* [12] with subsequent phase transition He I \rightarrow He vapor. In all probability the formation of the second temperature peak is caused by these processes.

As for the third peak, since its presence or absence depends on specimen orientation, the hydrodynamics of the interaction of the He I formed in the annular channel with the surrounding He II volume may be its cause.

Thus, the first temperature peak is probably related to development of superfluid turbulence in the He II, the second, to an He II \rightarrow He I transition in the metastable region, and the third, to the dynamics of removal of the He I formed from the annular channel. In all probability these processes also cause the accelerated (compared to free flow conditions) transition to film boiling.

At present experimental methods for verification of the proposed interpretations are being developed.

NOTATION

A, superheat peak amplitude, K; B, constant in Eq. (1), $\text{W}^4 \cdot \text{cm}^{-8} \cdot \text{sec}$; C, constant in Eq. (2), $\text{W}^{3/2} \cdot \text{cm} \cdot \text{sec}$; G, superheat peak half-width, sec; P, pressure, Pa; q, heat flux density, $\text{W} \cdot \text{m}^{-2}$; R, electrical resistance, Ω ; h, Kapitza conductivity, $\text{W} \cdot \text{m}^{-2} \cdot \text{K}^{-1}$; T, temperature, K; $\Delta T = T - T_s$, superheat, K; t, time, sec; W, pulse power, W; τ , time of superheat peak onset, sec. Subscripts: vx, vortex formation; cr, crisis; ss, steady state regime; λ , lambda point; s, saturation line.

LITERATURE CITED

1. S. K. Nemirovskii, *Inzh.-Fiz. Zh.*, 43, No. 4, 676-692 (1982).
2. P. Seyfert, *Proc. ICCC9, Guildford* (1982), pp. 263-268.
3. S. W. Van Sciver, *Adv. Cryog. Eng.*, 27, 375-398 (1982).
4. S. Patterman, *Hydrodynamics of Superfluid Liquid* [Russian translation], Moscow (1978).
5. V. F. Vinen, *Progr. Low Temp. Phys.*, 3, 1-57 (1961).
6. R. Airy, *Heat Transport at Low Temperatures* [Russian translation], Moscow (1977).
7. N. S. Snyder, *Cryogenics*, 10, No. 2, 89-95 (1970).
8. V. M. Miklyaev, V. F. Minashkin, S. Yu. Selyunin, et al., *Pr. XIII International Conference on Accelerators*, Vol. 2 [in Russian], Novosibirsk (1987), pp. 53-58.
9. J. A. Katerberg and A. C. Anderson, *J. Low-Temp. Phys.*, 42, Nos. 1/2, 165-176 (1981).

* The phase transition He II \rightarrow He I occurs in the metastable region, since the pressure at the surface of the heater-thermometer (with consideration of hydrostatics) is about 2140 Pa, which is significantly below $P_\lambda = 5036 \text{ Pa}$.